Supplementary Material

Electrocatalytic Hydrodechlorination Using Supported Atomically Precise Gold Nanoclusters under Flow-Through Configuration

Zhiyuan Zhao [1], Haochen Yan [2], Fuqiang Liu [2], Jie Yao [1], Shijie You [1,*] and Yanbiao Liu [2,3,*]

[1] State Key Laboratory of Urban Water Resource and Environment, School of Environment, Harbin Institute of Technology, Harbin 150090, China; 19bg29093@stu.hit.edu.cn (Z.Z.); yaojiejiehit@163.com (J.Y.)
[2] College of Environmental Science and Engineering, Donghua University, Shanghai 201620, China; 2212135@mail.dhu.edu.cn (H.Y.); liufuqiang@stu.ecnu.edu.cn (F.L.)
[3] Shanghai Institute of Pollution Control and Ecological Security, 1239 Siping Road, Shanghai 200092, China
* Correspondence: sjyou@hit.edu.cn (S.Y.); yanbiaoliu@dhu.edu.cn (Y.L.); Tel.: +86-21-67798752 (Y.L.)

Supplementary Material: 3 Texts and 10 Figures.

Table of Content

Text S1 DFT calculations

All the DFT calculations were conducted based on the Vienna Ab-inito Simulation Package (VASP).[1, 2] The exchange-correlation energy is processed by generalized-gradient approximation (GGA) in the form of Perdew-Burke-Ernzerhof (PBE) with spin polarization.[3, 4] The core-valence interactions were accounted by the projected augmented wave (PAW) method. The energy cutoff for plane wave expansions was set to 420 eV. To avoid interaction between layers, the vacuum layer is set to 20Å. The structural optimization was completed for energy and force convergence set at 1.0×10^{-5} eV and 0.01 eV $Å^{-1}$, respectively. The Brillouin zone 2 × 2 × 2 meshes for structural optimization. Grimme's DFT-D3 methodology was used to describe the dispersion interactions.[5]

According to the computational hydrogen electrode (CHE) model, the Gibbs free energy change (ΔG) for each elemental step was calculated by:

$$\Delta G = \Delta E + \Delta \mathrm{ZPE} - T\Delta S$$

where ΔE is the electronic energy difference directly obtained from DFT calculations, ΔZPE is the zero-point energy difference, T is the room temperature (298.15 K) and ΔS is the entropy change.

Text S2 LC-MS method

For the determination of reduction products, UPLC-Q-TOF MS/MS technique equipped with a BEH C18 column (150 mm × 3.0mm i.d., 1.7 μm; Waters, Milford, USA) to separate organic compounds was used. The column temperature was maintained at 30 °C, the gradient mobile phase ratio of A/B was set as: in the first 2 min, the ratio was kept at 95/5, then changed linearly from 95/5 to 0/100 in the next 3 min and held for 3 min, followed by a sharp decline to 95/5 in 0.05 min, and kept for 1.95 min for re-equilibration, where A is ammonium acetate and B is acetonitrile with the flow rate of 0.3 mL/min. The MS and MS/MS spectra of reduction products were analyzed in a molecular ion scanning mode in negative ESI mode. The data processing was conducted in DataAnalysis software (Agilent, American) according to the standard procedure.

Text S3 Catalyst characterizations

The morphology of the AuNC@CNT nanohybrid filter was characterized by FESEM. As shown in **Figure S1a**, the AuNC@CNT nanohybrid filter showed uniform porous microstructure with pore size of ~100 nm. However, it could be noted that superfluous Au nanoparticles lead to aggregation due to the reduction effect of applied negative potential (**Figure S1b**). The combination of AuNC with CNTs was further examined by TEM. **Figure S2** showed the diameter of the multiwall CNTs was 15 ± 3 nm. The AuNC were uniformly distributed on the surface of the CNTs. This data provided supportive evidence for the successful loading of AuNC onto CNTs. In order to further probe the chemical composition and their distribution, the EDS mapping for Au element were presented in **Figure S3**, which suggested the abundant distribution of Au on supports. In addition, by studying the thermal gravimetric analysis (TGA) spectra of AuNC@CNT nanohybrid filter, the amount of loaded AuNC was determined to be 2.1 ± 0.4 mg at an adsorption time of 90 min (**Figure S4**). Therefore, these results suggested the successful preparation of AuNC@CNT nanohybrid filter.

To better understand the chemical composition of AuNC@CNT nanohybrid filter, the comparison of the XPS survey spectrums of CNT and AuNC@CNT were obtained (**Figure S5a**). As shown in **Figure S5b**, two pairs of Au 4f spin−orbit coupling doublets were observed, with the $4f_{5/2}$ and $4f_{7/2}$ centred at 87.6 and 83.9 eV. These two peaks could be further deconvoluted into Au(0) (Au $4f_{5/2}$ peak at 87.4 eV and Au $4f_{7/2}$ peak at 84.2 eV) and Au(I) (Au $4f_{5/2}$ peak at 88.4 eV and Au $4f_{7/2}$ peak at 84.7 eV),

suggesting oxidation states of Au in $Au_{25}(MHA)_{18}$ NCs were a combination of 0 and 1.[6] The EIS was applied to characterize the charge transfer resistance (R_{CT}) of AuNC@CNT nanohybrid filter. **Figure S6** showed that a remarkably smaller radius of the circular arc associated with AuNC@CNT electrode (R_{CT} = 25 Ω) when compared to the non-Au-loaded CNT electrode (R_{CT} = 50 Ω). This could be attributed to the loading of AuNC significantly decreased the interfacial resistance as well as accelerating the electron transfer kinetics.

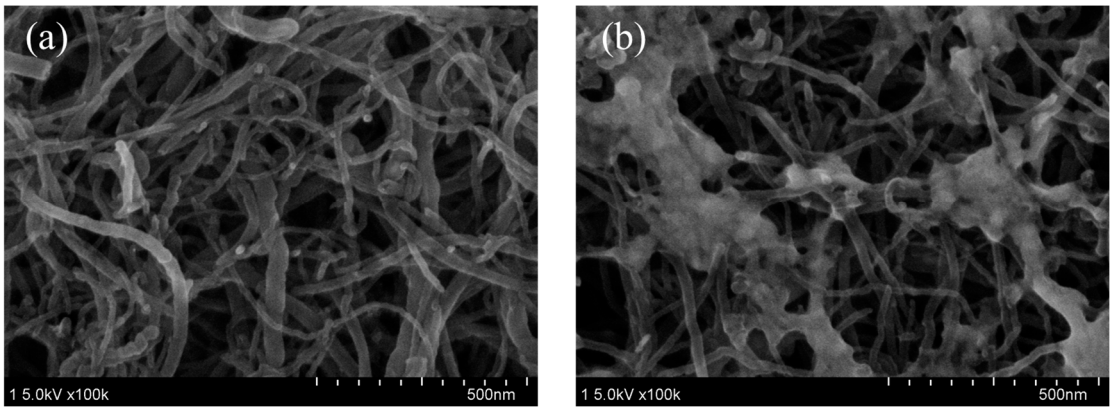

Figure S1. FESEM image of (a) AuNC@CNT and (b) agglomerated AuNC@CNT.

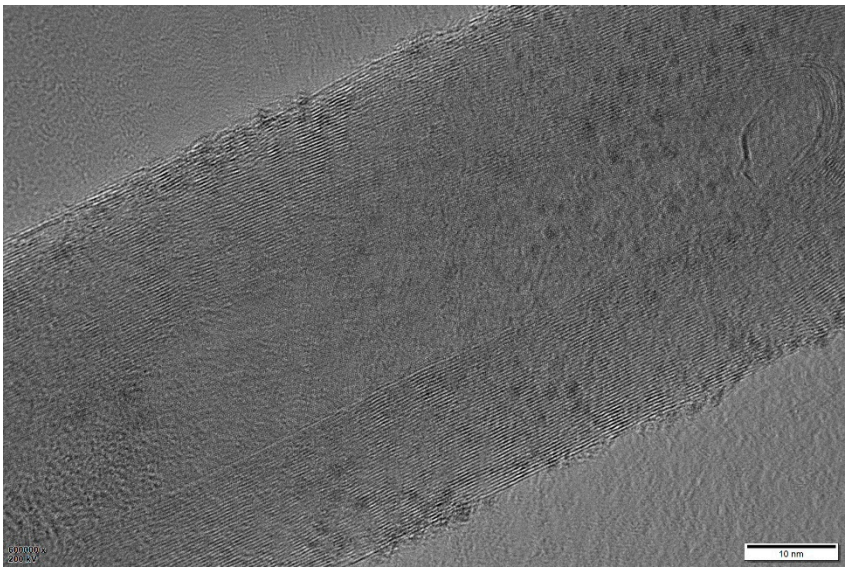

Figure S2. TEM images of AuNC@CNT.

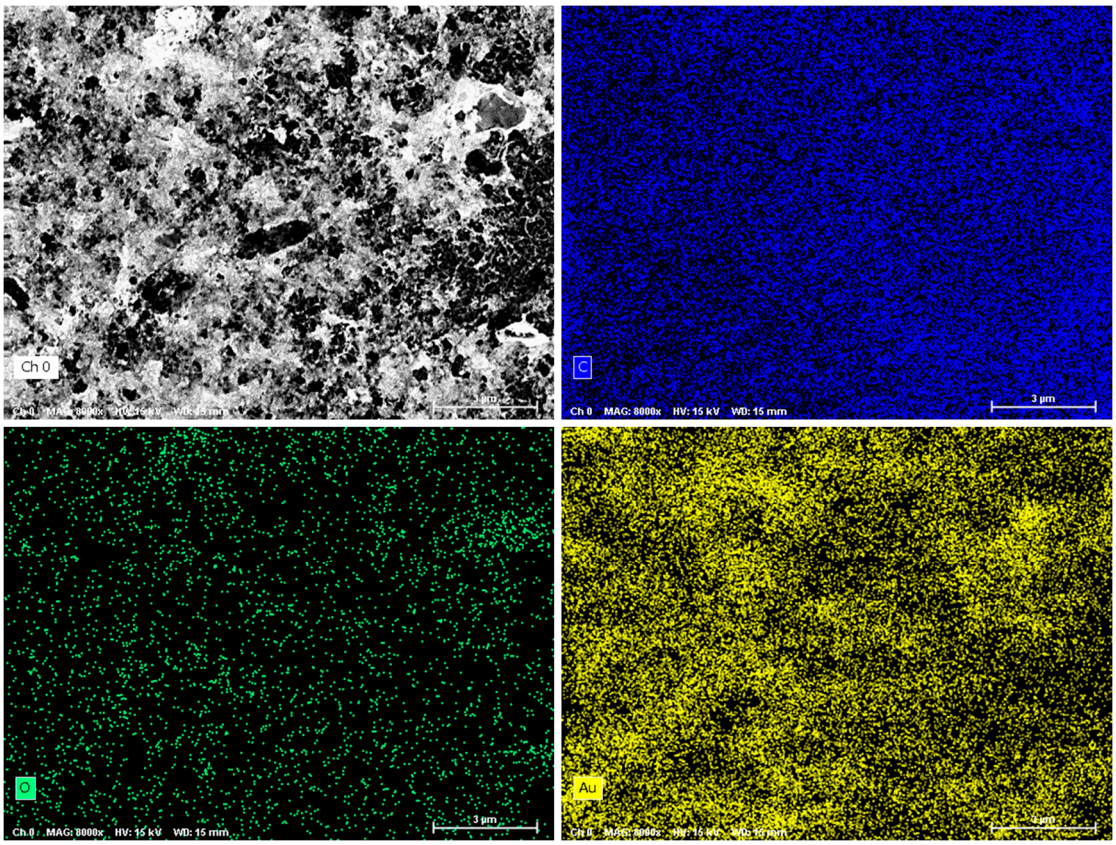

Figure S3. FESEM-EDS mapping images of AuNC@CNT.

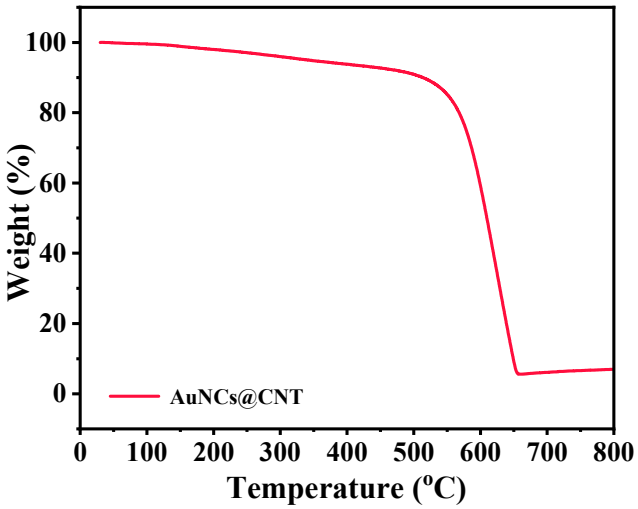

Figure S4. TGA curve of AuNC@CNT nanohybrid filter

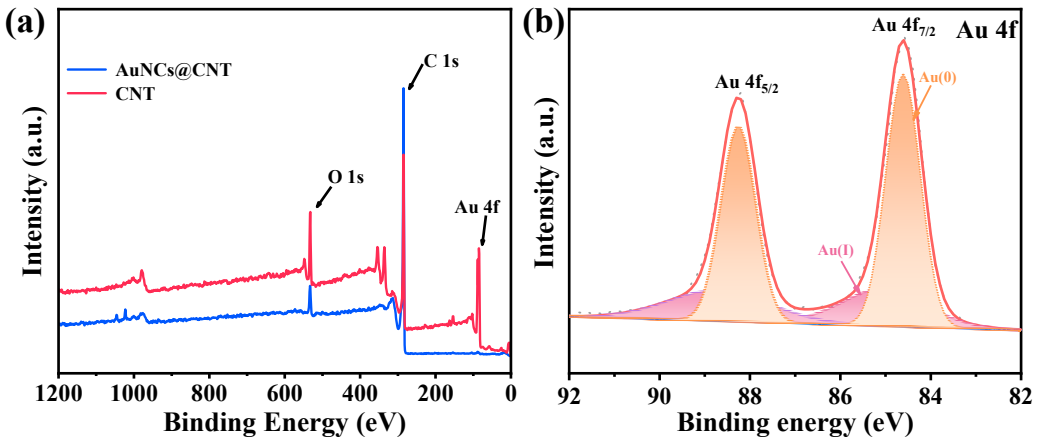

Figure S5. (a) Comparison of the XPS survey spectrums of CNT and AuNC@CNT; (b) High resolution Au 4f XPS spectrum of AuNC@CNT.

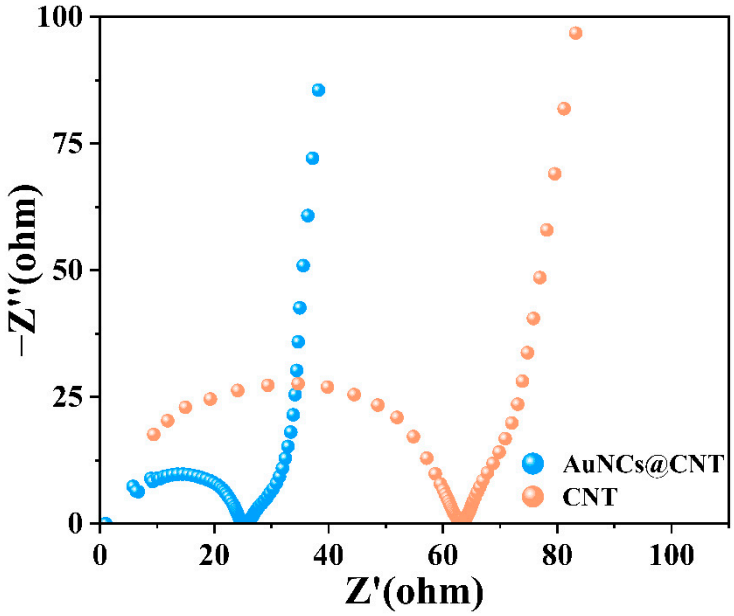

Figure S6. EIS spectra of the AuNC@CNT.

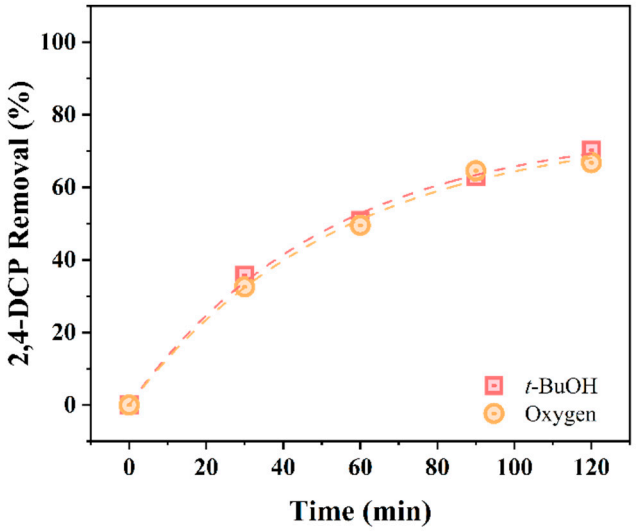

Figure S7. Comparison of 2,4-DCP removal using different quenching agents

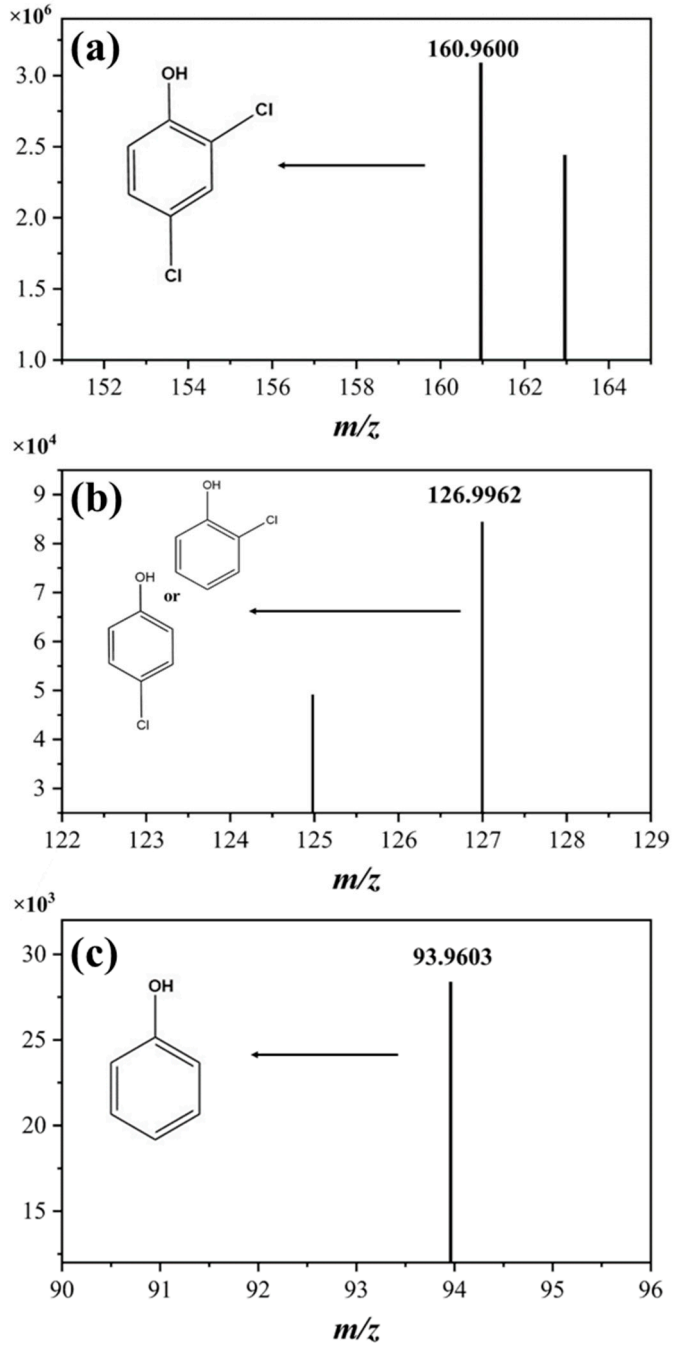

Figure S8. The MS spectra of (a) *m/z* = 160.9600, (b) *m/z* = 126.9962, (c) *m/z* =93.9603.

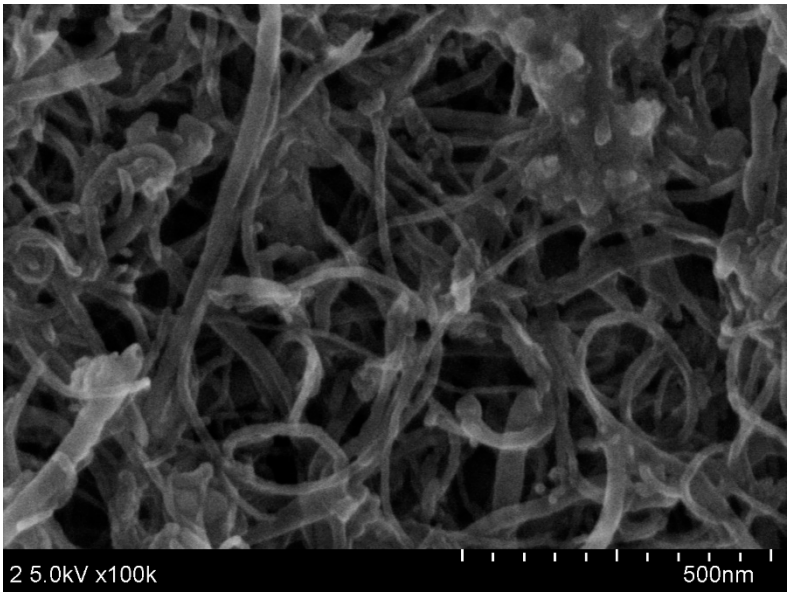

Figure S9. FESEM image of the AuNC@CNT after reaction.

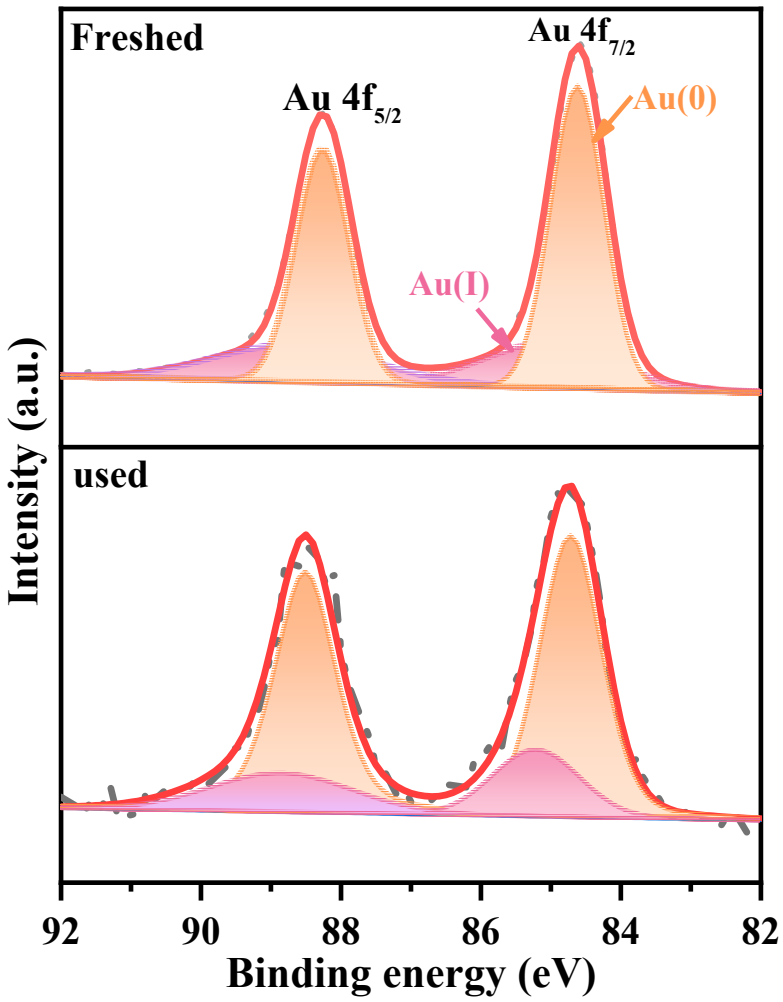

Figure S10. Comparison of the XPS survey spectrums of the Au 4f before and after reaction.

References

1. Kresse, G.; Hafner, J., Ab initio molecular dynamics for liquid metals. *Phys. Rev. B Condens Matter* **1993,** *47*, (1), 558-561.
2. Kresse, G.; Hafner, J., Ab initio molecular-dynamics simulation of the liquid-metal-amorphous-semiconductor transition in germanium. *Phys. Rev. B Condens Matter* **1994,** *49*, (20), 14251-14269.
3. Perdew, J. P.; Burke, K.; Ernzerhof, M., Generalized gradient approximation made simple. *Phys. Rev. Lett.* **1996,** *77*, (18), 3865-3868.
4. Kresse, G.; Joubert, D., From ultrasoft pseudopotentials to the projector augmented-wave method. *Phys. Rev. B.* **1999,** *59*, (3), 1758-1775.
5. Grimme, S.; Antony, J.; Ehrlich, S.; Krieg, H., A consistent and accurate ab initio parametrization of density functional dispersion correction (DFT-D) for the 94 elements H-Pu. *J. Chem. Phys.* **2010,** *132*, (15), 154104.
6. Liu, Y.; Zheng, Y.; Du, B.; Nasaruddin, R. R.; Chen, T.; Xie, J., Golden carbon nanotube membrane for continuous flow catalysis. *Ind. Eng. Chem. Res.* **2017,** *56*, (11), 2999-3007.
7. Fu, W.; Wang, K Zhou, Y.; Zhou, J.; Xia, S.; Rittmann, B. E., A kinetic model for 2,4-dichlorophenol adsorption and hydrodechlorination over a palladized biofilm. *Water Res.* **2022,** *214*, 118201.
8. Fu, W.; Wang, K.; Lv, X.; Fu, H.; Dong, X.; Chen, L.; Zhang, X.; Jiang, G., Palladium nanoparticles assembled on titanium nitride for enhanced electrochemical hydrodechlorination of 2,4-dichlorophenol in water. *Chin. J. Catal* **2018,** *39*, (4), 693-700.
9. Jiang, G.; Lan, M.; Zhang, Z.; Lv, X.; Lou, Z.; Xu, X.; Dong, F.; Zhang, S., Identification of active hydrogen species on palladium nanoparticles for an enhanced electrocatalytic hydrodechlorination of 2,4-dichlorophenol in water. *Environ. Sci. Technol.* **2017,** *51*, (13), 7599-7605.
10. Fu, W.; Shu, S.; Li, J.; Shi, X.; Lv, X.; Huang, Y.-X.; Dong, F.; Jiang, G., Identifying the rate-determining step of the electrocatalytic hydrodechlorination reaction on palladium nanoparticles. *Nanoscale* **2019,** *11*, (34), 15892-15899.
11. Shen, Y.; Tong, Y.; Xu, J.; Wang, S.; Wang, J.; Zeng, T.; He, Z.; Yang, W.; Song, S., Ni-based layered metal-organic frameworks with palladium for electrochemical dechlorination. *Appl. Catal. B* **2020,** *264*, 118505.